



UNIVERSITÀ DI PARMA

ARCHIVIO DELLA RICERCA

University of Parma Research Repository

CFD modeling of additive manufacturing liquid cold plates for more reliable power press-pack assemblies

This is the peer reviewed version of the following article:

Original

CFD modeling of additive manufacturing liquid cold plates for more reliable power press-pack assemblies / Cova, P.; Santoro, D.; Spaggiari, D.; Portesine, F.; Vaccaro, F.; Delmonte, N.. - In: MICROELECTRONICS RELIABILITY. - ISSN 0026-2714. - 114:(2020), p. 113734. [10.1016/j.microrel.2020.113734]

Availability:

This version is available at: 11381/2881746 since: 2024-10-25T18:05:42Z

Publisher:

Elsevier Ltd

Published

DOI:10.1016/j.microrel.2020.113734

Terms of use:

Anyone can freely access the full text of works made available as "Open Access". Works made available

Publisher copyright

note finali coverpage

(Article begins on next page)

CFD Modelling of Additive Manufacturing Liquid Cold Plates for More Reliable Power Press-Pack Assemblies

P. Cova^a, D. Santoro^a, D. Spaggiari^a, F. Portesine^b, F. Vaccaro^b, N. Delmonte^a

^a Dipartimento di Ingegneria e Architettura, University of Parma, Italy

^b POSEICO S.p.A., Genova, Italy

Abstract – In this work a new concept of liquid cold plate for high power press-pack assemblies is investigated. In industrial applications it is very important to reduce the volume and weight of the device-heatsink stack, in order to improve reliability and availability of the whole system. The potential of aluminum additive manufacturing technology is investigated by means of coupled thermal fluid-dynamic 3D modelling in order to get the best trade-off between thickness, thermal performance, and pressure drop. The validation of the numerical model was conducted by means of thermal characterization of a prototype with a properly built test bench. The numerical model was used to explore different solutions for the cold plate internal layout, such as with classical coils, deformed coils, or specific textures impossible with standard mechanical machining. Early results are shown to demonstrate the usefulness of our coupled thermal fluid-dynamic approach. Mechanical analysis was also taken into consideration, to account for possible weakness induced by the reduction in metal content typical of the advanced structures built with additive technology.

1. Introduction

The main hold up in power systems design is nowadays thermal management. Water cold plates are a key issue in many power electronics systems in order to develop reliable applications, especially when press-pack high power devices have to be cooled down. Maintaining a controlled temperature on power devices is a reliability key issue and for this reason an optimized design of liquid heatsinks is crucial.

In this work the use of Additive Manufacturing (AM) technology [1] for the fabrication of aluminum liquid cold plates for press-pack applications is investigated. AM enables the creation of a new generation of cooling systems and to overcome the limits of traditional manufactured cold plates, allowing better performances thanks to the optimization of the internal channels. Its use is promising, due to several advantages: the possible creation of multiple shapes of heatsinks each optimized and customized for the application; the possible increase of the dissipated power per unit of surface with consequent reduction of weight, costs and dimensions; the possible creation of high-performance heat exchangers in small customized series contexts as required in power electronics applications.

Moreover, AM presents various benefits that improve the reliability and availability of power systems using liquid cold plates in press-pack stacks. In fact: potential leakage risks are eliminated due to absence of welding; a better process efficiency can be obtained; the surface temperature is more uniform due to proper design of the inner structure; the stress of moving parts is reduced due to smaller and lighter stacks.

Fig. 1 presents two possible structures of cold plates fabricated by AM.

1.1 Potential and limitations of metal AM technology

Metal laser AM has become very attractive for industry applications. It enables the process of making products and components, such as heat-sinks, layer-by-layer from a digital CAD model. This kind of method, based on localized melting of metallic powder by a laser beam, offers a rapid manufacture, flexible parameters selection and the possibility of creating complex, delicate and highly customized pieces, that could not be created with the traditional methods and instruments, only few years ago [2-5].

Even though AM represents an interesting and cutting-edge production technology, it is characterized by some critical aspects and potential problems of the final pieces. In fact, porosity and cracks due to production imperfections, mechanical stresses and grain boundaries may occur.

First of all, a fine tuning of the laser parameters and an adequate choice of the suitable powder are required: some metal alloys (e.g. W-6Ta, aluminum alloys, etc.) are less characterized by grain boundaries and cracks than others [6,7].

Secondarily, pores in the final piece that can derive from lacks of fusion, solidification defects or gas production, could generate cracks and must be avoided. Heat treatment applications of the final pieces, with temperatures higher than 1000 °C, combined with a treatment based on isostatic pressure (of about 1 kbar), can significantly reduce that kind of failure mechanism, deriving from the reduced strength of the pores [7,8]. Eventually, the thermal treatment can also relieve residual stresses in the manufactured parts, limiting again the risk of cracks [5].

1.2 Prototyping and CFD modeling approach

The additive deposition process that has been used to produce the prototypes for this work is called Selective Laser Melting. It is a rapid prototyping technique for AM, in which a high power density laser is used to melt metal powders together to deposit a layer. The material used to build the samples is an AlSi10Mg alloy, with a deposition layer height of 30 μm or 50 μm. It was noted that the paste with a deposition height of 30 μm was better from a qualitative point of view but more expensive and with longer processing times. The main limitations of this techniques are:

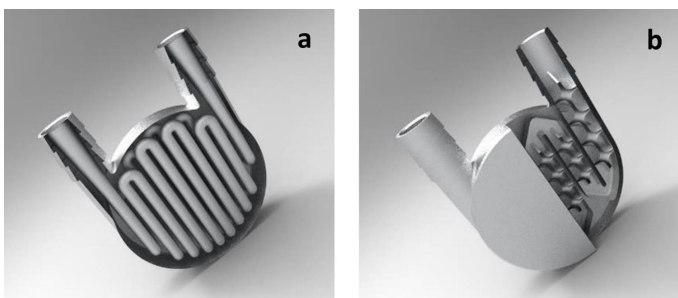


Fig. 1. Two possible internal structures manufacturable by additive technology.

- Not optimal finishing and printing of the holes;
- Finishing and printing of long overhanging surfaces;
- Support structures during the process;
- A metal cannot be printed on a different one;
- The thread cannot be used;
- Still excessive cost and excessive manufacturing time;
- Excessive cost of machinery;
- Currently, a limited amount of alloys can be used.

The great amount of degrees of freedom made available by this technology collides with the need to limit the pressure drop, one of the main constraints imposed by the cooling facility. For this reason, and due to the limitations above reported, instead of using manual procedures that require the fabrication of several prototypes to get the best solution [9], coupled Finite Element Method (FEM) Computational Fluid-Dynamic (CFD) analysis can be effectively used, as reported in [10,11]. In this paper we show the effectiveness of this modeling approach for an application driven optimum design of aluminum cold plates, in term of thermal resistance, pressure drop, and surface temperature uniformity.

Section 2 illustrates the test bench that was properly set up to perform thermal measurements on a cold plate prototype, needed for tuning the numerical model. Section 3 describes our FEM-CFD model and its tuning by the thermal measurement performed on the prototype. In section 4 examples of cold plates design are shown, together with the analysis of the simulation results. Finally, mechanical analysis was taken into account, and shown in Section 5, in order to verify the compliance with the clamping force constraint in press-pack assemblies. Section 6 draws the conclusions.

2. Test Bench for Thermal Measurements

Fig. 2 shows the test bench set up to perform thermal measurements on a cold plate prototype with known inner structure, in order to tune and validate the numerical model. It is composed by a water open circuit with valves and a flowmeter, a Flir A325 IR camera, thermometers with some thermocouples,

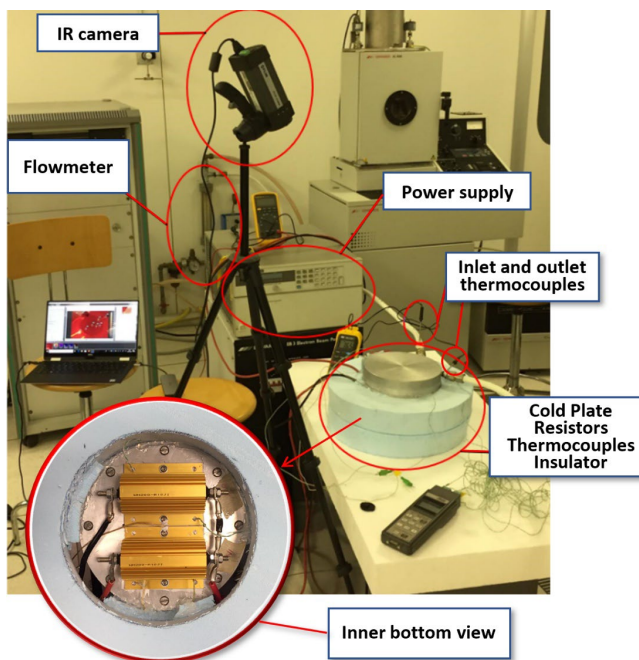


Fig.2. Test bench for thermal characterization.

a power supply, and an aluminum cold plate with 0.1Ω power resistors on one side. The power resistors are accurately mounted on the cold plate by means of a thermal paste in order to minimize the thermal contact resistance. The top side of the cold plate is kept clear to monitor its temperature. This surface was painted matt to have a uniform and high emission coefficient.

The cold plate is heated by the two power resistors ($P_{diss} = 200 \text{ W/each}$) well thermally insulated on the bottom side. The insulator was sized to have a negligible heat flow from resistors towards environment. Special care was paid to the electrical wiring and water pipes, so as not to induce heat loss through insulation. Therefore, the measured output power supplied can be considered the heat injected in the cold plate. To measure the temperature of the water at the inlet and at the outlet, two K type thermocouples were inserted in the pipes very close to the cold plate. Some other K type thermocouples were placed on the resistor side, to measure the temperature in points of interest where the IR camera cannot be used.

More details about the test bench can be found in [12].

3. Numerical Model Settings

The modeling has been done coupling The Heat Transfer in Solid and Fluid equations with the Laminar Flow equations of COMSOL Multiphysics 5.3. Fig. 3 shows the settings typically applied to simulate a cold plate solution.

The desired bilateral heat removal easily leads to design symmetric coolant paths. In this case, symmetries allow to reduce the study to a half, or a quarter of the whole heatsink, saving a lot of computing resources during simulations.

The heat transfer was modeled with the following settings: water as coolant; thermal properties of the metal taken by the datasheet of the cold plate manufacturer (additive or traditional technology); fixed temperature at the inlet; COMSOL Outflow condition (it is assumed that convection is the dominating transport mechanism across the outlet boundary, and therefore that diffusive transport can be neglected); a parametric inward heat flux at the faces that will be in contact with the electronic devices to cool; natural air convection at the boundaries exposed to the air. The CFD was modeled considering a parametric laminar inflow at the inlet and a reference pressure at the outlet.

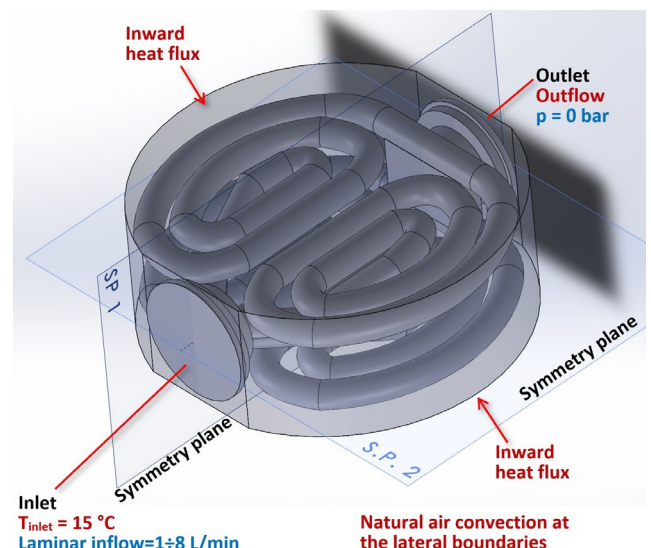


Fig. 3. FEM setup (cold plate with two symmetry planes).

At all other fluid boundaries (those in contact with the aluminum walls) a “no slip” condition was set.

In order to tune and validate the model, simulations of the cold plate used for thermal characterization in the test bench described in Section 2 were conducted. The simulation results were then compared with those of the measurements at the same operating conditions. The comparison was done on the basis of the temperature map acquired by the IR camera and the temperatures measured by the thermocouples on the cold plate and on the water outlet. The only fitting parameter used for tuning the model was the thermal exchange coefficient, which accounts for air convection and radiation on the lateral vertical walls, even though its relevance is poor in press-pack assembly.

After comparing simulation and measurement results at different values of input power and flow rate, the thermal exchange coefficient was fixed to $h_T = 7.06 \text{ W/m}^2\text{K}$. In the whole set of operating conditions the maximum absolute error was below than $1 \text{ }^\circ\text{C}$. Therefore, we can consider the model accurate enough to use it to analyze different internal structures. Fig. 4 shows, as an example, the comparison between simulated and measured temperature map on the cold plate free surface with an input power of 400 W, an inlet water temperature of $15.5 \text{ }^\circ\text{C}$ and a flow rate of 2 l/min.

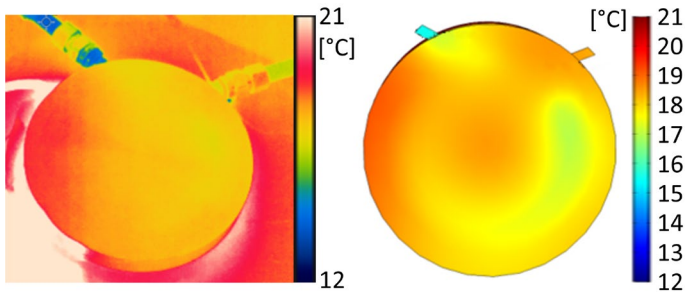


Fig. 4. Temperature map ($^\circ\text{C}$) of the prototype free surface measured by IR camera (left) and simulated after model tuning (right) at the same operating conditions: $T_{\text{inlet}} = 15.5 \text{ }^\circ\text{C}$, flow rate = 2 l/min, $P_{\text{diss}} = 400 \text{ W}$.

4. Simulation Results and Discussion

The most significant variables to qualify the behavior of the designed cold plates are the surface temperature (in term of maximum value and uniformity) and the pressure drop at a given flow rate. Indeed the pressure drop is an important limitation factor, because it represents the load for the water conditioning system pumps, which usually have to drive various cold plates in series. Typical values acceptable for a single cold plate are below few hundreds mbar, depending on the flow rate.

Various internal layouts were simulated and many more are possible. The most promising structures, will be shown in this section together with the simulation results, in term of surface temperature map and pressure drop. All the structures that will be shown feature a thickness of 11 mm.

4.1 “Twice Coil” cold plate

Fig. 5 illustrates the 3D model of the inner layout of the prototype of Fig. 1.a, with a “Twice Coil” structure, and the main operating conditions of the simulations performed.

Fig. 6 shows the simulated surface thermal map simulated for this cold plate, compared at the same operating conditions with that of the standard technology cold plate that we used for

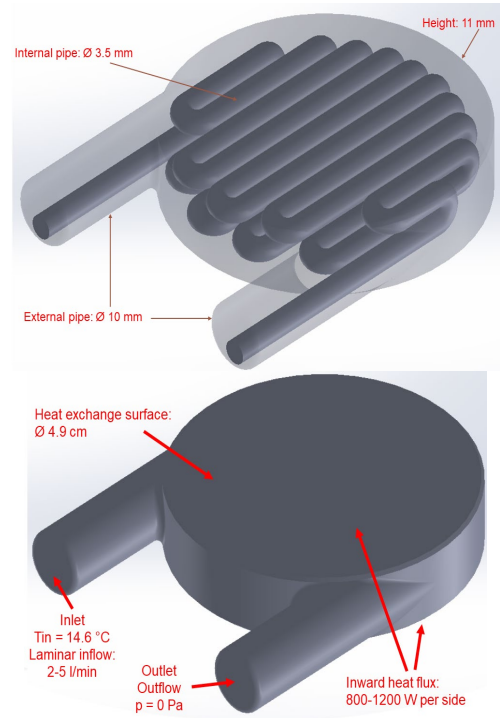


Fig. 5. 3D model of the inner layout (top) and simulation operating conditions (bottom) for the cold plate of Fig. 1.a.

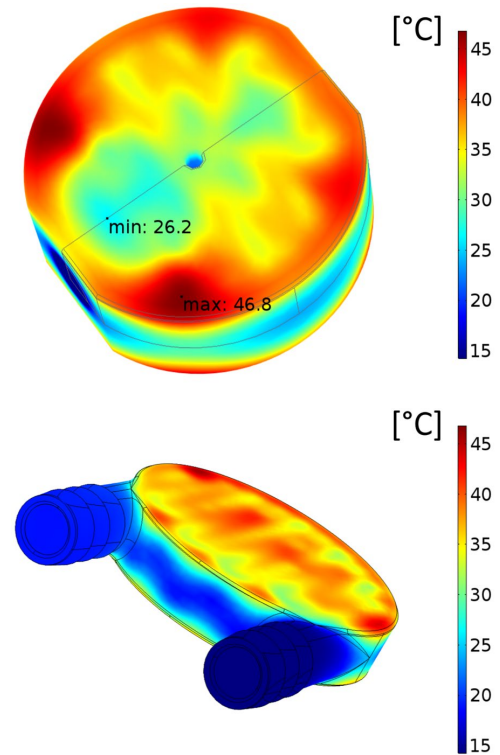


Fig. 6. Temperature map simulated with a standard technology cold plate (top) and with the structure “Twice Coil” (bottom). $T_{\text{inlet}} = 15 \text{ }^\circ\text{C}$, flow rate = 5 l/min, $P_{\text{diss}} = 800 \text{ W}$ each side.

thermal characterization. Although the maximum surface temperature is similar, the temperature uniformity is much higher with the new design. Moreover, the “Twice Coil” cold plate is 11 mm thick, versus 22 mm of the standard cold plate, and has a weight of 40 g, against 160 g of the latter. However, this structure is not exploitable form common water conditioning systems due to the too high pressure drop.

4.2 “Mixer” cold plate

A more promising structure was the so-called “Mixer”, very similar to the one shown in Fig. 1.b, which is obtained by adding many properly shaped inner bumps to a larger conventional coil. These bumps are used for a water “mixing” function. Fig. 7 shows the inner layout of this cold plate, which enables a twice improvement in the heat exchange between fluid and metal. In fact, the surface area is increased, and vorticity is induced, which in turn increases the heat exchange coefficient because it tends to remove the layer of unmoved fluid in contact with the aluminum wall, typical in laminar flow.

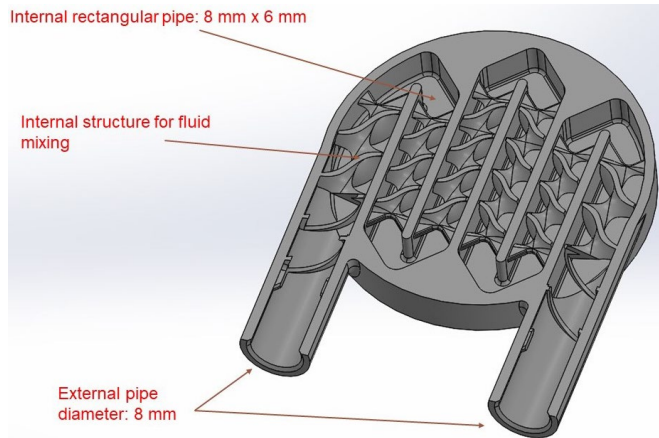


Fig. 7. 3D model of the inner layout of the “Mixer” cold plate.

The simulation conditions were the same reported in Fig. 5. Fig. 8 shows the temperature maps with a flow rate of 2 l/min and 5 l/min, in case of a heat flux of 1200 W per side. The results in terms of surface temperature map are very good, in comparison with that shown in Fig. 6 for the “Twice Coil” prototype dissipating 800 W per side with a flow rate of 5 l/min. The pressure drop in the “Mixer” cold plate is 450 mbar, close to acceptable values, with a flow rate of 2 l/min, but dramatically increases above 2 bar (not acceptable) with a flow rate of 5 l/min.

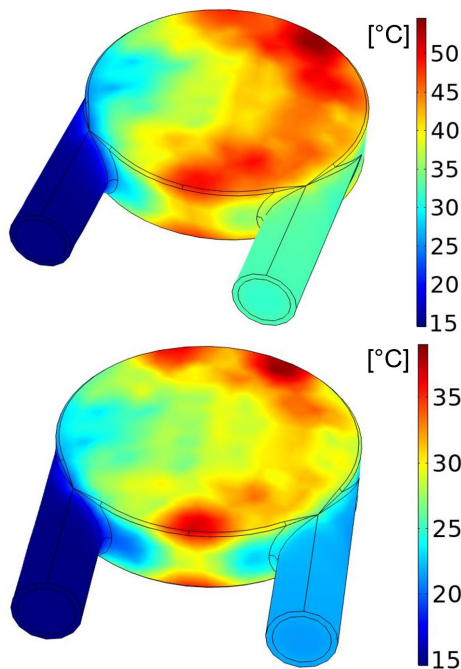


Fig. 8. Thermal map simulated for the “Mixer” structure flow rate of 2 l/min (top) and 5 l/min (bottom). $T_{inlet} = 15\text{ }^{\circ}\text{C}$. $P_{diss} = 1200\text{ W}$ per side.

4.3 “Ram” cold plate

A third example of structure manufacturable only by additive technology is the one we called “Ram” cold plate, since its inner structure resembles the horns of a ram. The inner layout is shown in Fig. 9 together with the simulation conditions. In this case, both the surface temperature distribution and the pressure drop are compliant with requirements, as shown in Fig. 10, which shows the surface temperature map with flow rate of 5 l/min. In particular, the thermal performance of this structure is excellent, while the pressure drop is at the limit of the acceptable values.

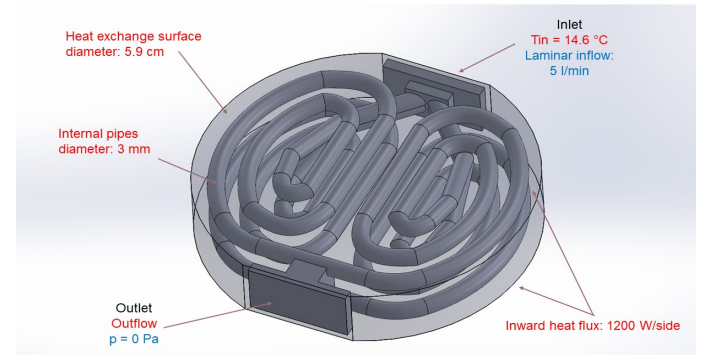


Fig. 9. 3D model of the inner layout of the “Ram” cold plate and simulation operative conditions.

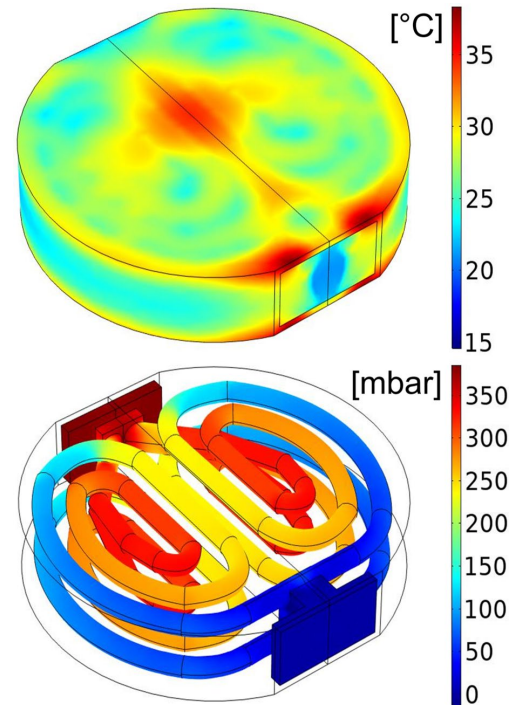


Fig. 10. Surface temperature map (top) and pressure along the coil (bottom) simulated for the “Ram” cold plate. $T_{inlet} = 15\text{ }^{\circ}\text{C}$, flow rate = 5 l/min, $P_{diss} = 1200\text{ W}$ per side.

4.4 “Grid” cold plate

The last structure that will be described in this paper is the so called “Grid” cold plate, since it combines an almost usual coil with orthogonal pipes, properly shaped in order to optimize the velocity profile over the water paths. The inner structure layout, together with the simulation conditions, is depicted in Fig. 11.

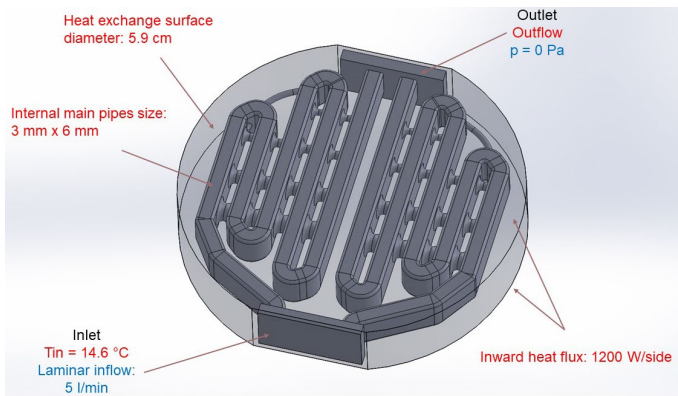


Fig. 11. 3D model of the inner layout of the “Grid” cold plate and simulation operative conditions.

Fig. 12 shows, in the case of a flow rate of 5 l/min, the water velocity, the surface temperature map, and the pressure in the water. It can be observed that in this case the thermal performances are similar to that of the “Twice Coil” cold plate, but the pressure drop is lowered to the excellent value of 170 mbar.

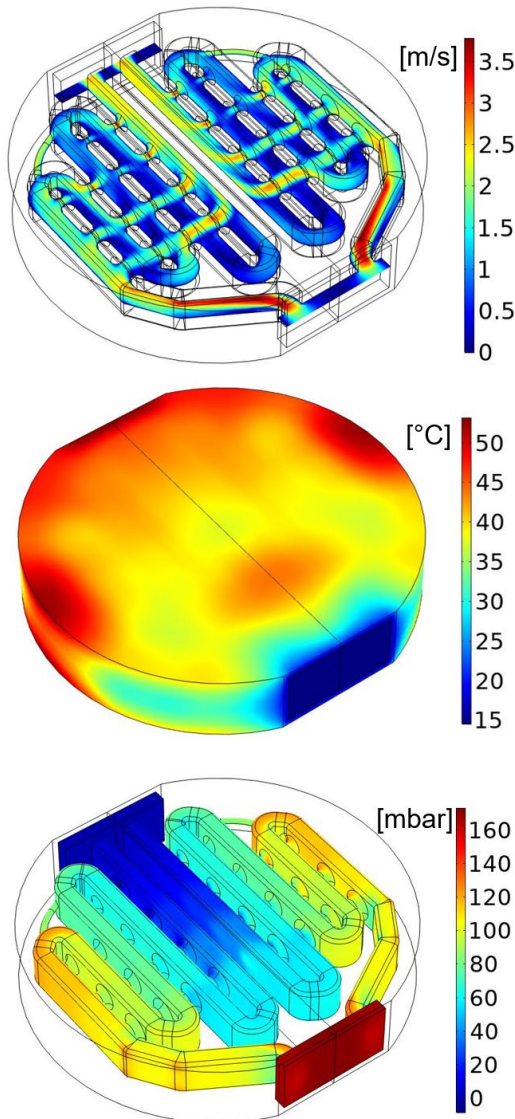


Fig. 12. Water velocity (top), surface temperature map (center) and pressure along the coil (bottom) simulated for “Grid” cold plate. $T_{inlet} = 15$ °C, flow rate = 5 l/min, $P_{diss} = 1200$ W per surface.

5. Mechanical Simulations

An important issue to take into account in cold plates for press-pack assembly application is the mechanical robustness, especially when the metallic structure is thinned and lightened, reducing the metal content in favor of the volume of water, as it happens with the structures made with AM technology.

By exploiting the COMSOL Structural Mechanics module, we performed mechanical simulations in the elastic regime, calculating the Von Mises stress and total displacement over the whole cold plate, by applying a total clamping force of 30 kN, a typical value for press pack assemblies.

For all the designed structures the value of the mechanical stress was about three orders of magnitude below the Young module of the material and the maximum deformation was in the order of few μm , comparable with the surface roughness. Therefore, we can predict that the designed structures will be mechanically compliant with using in press-pack applications. Fig. 13 shows an example of the simulation results for the “Grid” structure.

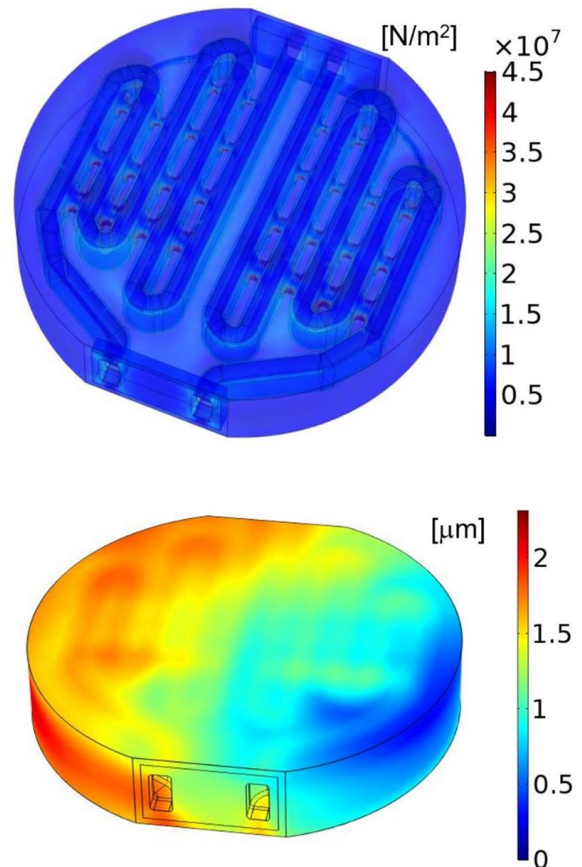


Fig. 13. Von Mises stress (top) and deformation (bottom) simulated for the “Grid” structure with an external force 15 kN per side. $T = 20$ °C.

6. Conclusions

In this paper we demonstrate the need and effectiveness of a CFD modeling approach for designing innovative structures that exploit the potentiality of AM technology in the fabrication of a new generation of aluminum cold plates for application in power press-pack assemblies.

By this procedure, once tuned the numerical model, lighter and more reliable cold plates can be customized for every application and developed without need of prototypes.

Many innovative inner structures were designed and simulated by this approach. Promising results, both in term of surface temperature and pressure drop, were obtained with two of them and shown in this paper. Moreover, mechanical simulations were conducted as well for these structures, demonstrating the capability to withstand the typical operating clamping pressure in press-pack assemblies. Therefore, we demonstrated the suitability of the presented multi-physics modeling approach for designing cold plates manufacturable with AM technology for any specific application.

References

- [1] W.E. Frazier, Metal Additive Manufacturing: A Review, *J. of Mater Eng and Perform* 23 (2014) 1917-1928.
<https://doi.org/10.1007/s11665-014-0958-z>
- [2] K.K. Fletcher, T.E. Sparks, A. Flood, F. Liou, A SOA approach to improve performance of metal additive manufacturing simulation, 2017 IEEE International Conference on Cognitive Computing (ICCC), Honolulu, HI (2017) 140-143.
<https://doi.org/10.1109/IEEE.ICCC.2017.26>.
- [3] S.L. Lin, C.C. Lin, D.Y. Lin and C.S. Chuang, Laser additive manufacturing technology in titanium 64 implant of microstructure fabrication and analysis, The 8th Annual IEEE International Conference on Nano/Micro Engineered and Molecular Systems, Suzhou (2013) 594-597.
<https://doi.org/10.1109/NEMS.2013.6559801>.
- [4] Y. Yan, C. Ding, K.D. T. Ngo, Y. Mei, G. Lu, Additive manufacturing of planar inductor for power electronics applications, International Symposium on 3D Power Electronics Integration and Manufacturing (3D-PEIM), Raleigh, NC (2016) 1-16. <https://doi.org/10.1109/3DPEIM.2016.7570536>.
- [5] L. Yuan, Solidification defects in additive manufactured materials. *JOM* 71, (2019) 3221-3222. <https://doi.org/10.1007/s11837-019-03662-x>.
- [6] D. Wang, Z. Wang, K. Li, J. Ma, W. Liu, Z. Shen, Cracking in laser additively manufactured W: Initiation mechanism and a suppression approach by alloying. *Materials & design* 162 (2019) 384-393. <https://doi.org/10.1016/j.matdes.2018.12.010>.
- [7] F.H. Kim, S.P. Moylan, Literature review of metal additive manufacturing defects, NIST Advanced Manufacturing Series 100-16 (2018). <https://doi.org/10.6028/NIST.AMS.100-16>.
- [8] A. Riemer, H.A. Richard, Crack propagation in additive manufactured materials and structures, *Procedia Structural Integrity*, 2 (2016) 1229-1236.
<https://doi.org/10.1016/j.prostr.2016.06.157>.
- [9] S.G. Kandlikar, C.N. Hayner, Liquid cooled cold plates for industrial high-power electronic devices - thermal design and manufacturing considerations, *Heat Transfer Eng* 30 (2009) 918-930. <https://doi.org/10.1080/01457630902837343>.
- [10] P. Cova, N. Delmonte, F. Giuliani, M. Citterio, S. Latorre, M. Lazzaroni, A. Lanza, Thermal optimization of water heat sink for power converters with tight thermal constraints, *Microelectronics Reliability* 53 (2013) 1760-1765.
<https://doi.org/10.1016/j.microrel.2013.07.035>.
- [11] P. Cova, N. Delmonte, D. Chiozzi, M. Portesine, F. Vaccaro, E. Mantegazza, Water cold plates for high power converters: a software tool for easy optimized design, *Microelectronics Reliability* 88-90 (2018) 801-805.
<https://doi.org/10.1016/j.microrel.2018.06.050>.
- [12] M. Lazzaroni, M. Citterio, S. Latorre, A. Lanza, P. Cova, N. Delmonte, F. Giuliani, Metrological characterization of cold plates for power converters, *IEEE Trans. on Instrumentation and Measurement* 65 (2016) 37-45.
<https://doi.org/10.1109/TIM.2015.2479104>.